

# Vertex corrections to the polarizability do not improve the $GW$ approximation for molecules

Alan M. Lewis and Timothy C. Berkelbach\*

*Department of Chemistry and James Franck Institute, University of Chicago, Chicago, Illinois 60637, USA*

The  $GW$  approximation is based on the neglect of vertex corrections, which appear in the exact self-energy and the exact polarizability. Here, we investigate the importance of vertex corrections in the polarizability only. We calculate the polarizability with equation-of-motion coupled-cluster theory with single and double excitations (EOM-CCSD), which rigorously includes a large class of vertex corrections beyond the random phase approximation (RPA). As is well-known, the frequency-dependent polarizability predicted by EOM-CCSD is quite different (and generally more accurate) than that predicted by the RPA. However, when the vertex-corrected  $GW$  approximation is tested on a set of 20 atoms and molecules, it predicts ionization potentials that are only marginally different (and slightly worse) than those calculated when vertex corrections are neglected. This result suggests that vertex corrections in the self-energy cannot be neglected, at least for molecules. We also assess the behavior of eigenvalue self-consistency in vertex-corrected  $GW$  calculations, again finding a marginal worsening of the predicted ionization potentials.

## I. INTRODUCTION

The  $GW$  approximation<sup>1</sup> has been widely and successfully used to calculate the charged excitation energies associated with electron addition and removal. It has been applied to a variety of solids, including simple metals, semiconductors, and transition metal oxides,<sup>1–8</sup> and more recently to atoms and molecules.<sup>7,9–16</sup> Since its introduction, a number of attempts have been made to improve upon the  $GW$  approximation through the inclusion of diagrammatically-defined vertex corrections beyond the random phase approximation (RPA). In some cases, vertex corrections are found to improve the accuracy of predicted excitation energies.<sup>17–20</sup> However, in other cases, the lowest-order vertex corrections produce results that are only marginally different, in both the condensed phase<sup>21–26</sup> and in isolated molecules.<sup>14,15,27</sup>

Here, we implement a large class of infinite-order vertex corrections to the polarizability using equation-of-motion coupled-cluster theory with single and double excitations (EOM-CCSD). In addition to the particle-hole ring diagrams resummed by the RPA, EOM-CCSD includes particle-hole ladder diagrams, particle-particle ladder diagrams, exchange diagrams, and mixtures of all of the above. Furthermore, similar to the conventional implementation of the Bethe-Salpeter equations,<sup>28,29</sup> the propagator lines are dressed and particle-hole interactions are screened. We use this improved polarizability to construct a more accurate screened Coulomb interaction  $W$ , for use in the  $GW$  approximation; because this style of vertex corrections aims to calculate  $W$  in terms of the response of a test charge due to a test charge, it is sometimes referred to as  $G_0W^{tc-tc}$ . We assess this vertex-corrected  $GW$  approximation by calculating the ionization potentials of the twenty smallest atoms and molecules of the  $GW100$  test set, which has recently been introduced for the purpose of benchmarking different implementations of the  $GW$  approximation.<sup>12,13,15,16</sup> By comparing our results to those obtained using conventional RPA screening, we conclude that vertex corrections to the polarizability do not improve the accuracy of the  $GW$  approximation for molecules. We also implement eigenvalue self-consistency in our vertex-corrected  $GW$  calculations, and again find no improvement. We con-

clude that high-order vertex corrections to the self-energy are required to improve on existing methods.

## II. THEORY

Charged excitation energies, associated with electron addition and removal, are often calculated by finding the poles of the one-electron Green's function,

$$G(1, 2) = -i \langle \Psi_0 | T[\psi^\dagger(1)\psi(2)] | \Psi_0 \rangle. \quad (1)$$

Here  $\psi^\dagger$  and  $\psi$  are field operators, the labels 1 and 2 indicate a set of position and time variables,  $T$  is the time-ordering operator, and  $|\Psi_0\rangle$  is the ground state of the many-electron system. In practice,  $G$  is usually calculated via the self energy  $\Sigma$ , defined by the Dyson equation,

$$G(1, 2) = G_0(1, 2) + \int G_0(4, 2)\Sigma(3, 4)G(1, 3)d(3)d(4), \quad (2)$$

where  $G_0$  is a noninteracting or mean-field Green's function.

Following Hedin,<sup>1</sup> the exact self-energy may be written as

$$\Sigma(1, 2) = i \int G(1, 4)W(1, 3)\Gamma(4, 2, 3)d(3)d(4), \quad (3)$$

where  $W$  is the screened Coulomb interaction and  $\Gamma$  is a three-point vertex function. The screened Coulomb interaction is given by

$$\begin{aligned} W(1, 2) &= V(1, 2) + \int V(4, 2)\Pi^*(3, 4)W(1, 3)d(3)d(4) \\ &= V(1, 2) + \int V(4, 2)\Pi(3, 4)V(1, 3)d(3)d(4), \end{aligned} \quad (4)$$

where  $\Pi^*$  and  $\Pi$  are the proper and improper polarizabilities, defined via

$$\Pi^*(1, 2) = -i \int G(2, 3)G(4, 2)\Gamma(3, 4, 1)d(3)d(4). \quad (5)$$

The three-point vertex function  $\Gamma$  appearing in Eqs. (3) and (5) is defined by

$$\begin{aligned} \Gamma(1, 2, 3) &= \delta(1, 2)\delta(1, 3) \\ &+ \int G_0(4, 1)G_0(1, 5)\frac{\delta\Sigma(2, 3)}{\delta G_0(4, 5)}d(4)d(5). \end{aligned} \quad (6)$$

The conventional *GW* approximation follows by setting  $\Gamma(1, 2, 3) = \delta(1, 2)\delta(1, 3)$ , i.e. neglecting vertex corrections, leading to

$$\Sigma(1, 2) \approx iG(1, 2)W(1, 2), \quad (7)$$

$$\Pi^*(1, 2) \approx -iG(2, 1)G(1, 2). \quad (8)$$

In practice, the *GW* approximation is commonly implemented without self-consistency, where *G* and *W* are evaluated in a one-shot manner based on the mean-field starting point, leading to the so-called  $G_0W_0$  approximation.

The exact improper polarizability has a Lehmann representation

$$\begin{aligned} \Pi(1, 2) &= \langle \Psi_0 | T[\tilde{\rho}(1)\tilde{\rho}(2)] | \Psi_0 \rangle \\ &= \theta(t_1 - t_2) \sum_{n \neq 0} e^{-i\Omega_n(t_1 - t_2)} \rho_n(\mathbf{x}_1) \rho_n^*(\mathbf{x}_2) + (1 \leftrightarrow 2) \end{aligned} \quad (9)$$

where  $\tilde{\rho} = \rho - \langle \Psi_0 | \rho | \Psi_0 \rangle$ ,  $\rho = \psi^\dagger \psi$ ,  $\rho_n(\mathbf{x}) = \langle \Psi_0 | \rho(\mathbf{x}) | \Psi_n \rangle$ , and  $\Omega_n = E_n - E_0$ . Separating the *GW* self-energy into its exchange and correlation components gives

$$\Sigma^x(1, 2) = iG(1, 2)V(1, 2) \quad (10a)$$

$$\Sigma^c(1, 2) = iG(1, 2) \int V(4, 2)\Pi(3, 4)V(1, 3)d(3)d(4). \quad (10b)$$

In a finite single-particle basis, the frequency dependence can be treated analytically such that the correlation component of the self-energy is given by

$$\begin{aligned} \Sigma_{pq}^c(\omega) &= \sum_{\Omega_n > 0} \left[ \sum_i \frac{(pi|\rho_n^*)(\rho_n|i q)}{\omega - (\varepsilon_i - \Omega_n) - i\eta} \right. \\ &\quad \left. + \sum_a \frac{(pa|\rho_n)(\rho_n^*|aq)}{\omega - (\varepsilon_a + \Omega_n) + i\eta} \right] \end{aligned} \quad (11)$$

where

$$(pq|\rho_n) = \int d\mathbf{x}_1 \int d\mathbf{x}_2 \phi_p^*(\mathbf{x}_1) \phi_q(\mathbf{x}_1) |\mathbf{x}_1 - \mathbf{x}_2|^{-1} \rho_n(\mathbf{x}_2). \quad (12)$$

Here and throughout we use indices *i, j* to denote orbitals that are occupied and *a, b* to denote orbitals that are unoccupied in the mean-field reference determinant. Equation (11) provides the formalism by which any theory of the polarizability can be employed in the *GW* approximation. For example, conventional RPA screening (no vertex corrections), as defined by Eq. (8), is recovered if the transition moments  $\rho_n(\mathbf{x})$  and excitation energies  $\Omega_n$  are obtained from the familiar eigenvalue problem<sup>30</sup>

$$\begin{pmatrix} \mathbf{A} & \mathbf{B} \\ -\mathbf{B}^* & -\mathbf{A}^* \end{pmatrix} \begin{pmatrix} \mathbf{X} \\ \mathbf{Y} \end{pmatrix} = \begin{pmatrix} \mathbf{X} \\ \mathbf{Y} \end{pmatrix} \Omega, \quad (13)$$

where

$$A_{ia,jb} = (\varepsilon_a - \varepsilon_i) \delta_{ab} \delta_{ij} + \langle ib|a j \rangle, \quad (14a)$$

$$B_{ia,jb} = \langle ij|ab \rangle, \quad (14b)$$

and

$$\rho_n(\mathbf{x}) = \sum_{ai} [X_{ia}^n \phi_a(\mathbf{x}) \phi_i^*(\mathbf{x}) + Y_{ia}^n \phi_i(\mathbf{x}) \phi_a^*(\mathbf{x})]. \quad (15)$$

This flavor of RPA is sometimes referred to as “direct RPA” because it neglects the exchange integrals that would arise from antisymmetrization in Eqs. (14). If the antisymmetrized integrals are maintained, then the screening is equivalent to time-dependent Hartree-Fock (TDHF). This level of theory is used to implement vertex corrections in the recent work of Maggio and Kresse,<sup>15</sup> and will be discussed later.

Here, we implement vertex corrections in the polarizability by using EOM-CCSD transition densities and excitation energies in Eq. (11). The formalism rigorously subsumes RPA screening (no vertex corrections) and TDHF screening. Briefly, EOM-CCSD excitation energies are defined as eigenvalues of the similarity-transformed normal-ordered Hamiltonian  $H_N = e^{-T} H e^T - E_{\text{CCSD}}$  in the subspace of determinants that are singly and doubly excited with respect to a reference determinant  $|\Phi\rangle$ . The operator *T* creates single and double excitations,  $T = \sum_{ai} t_i^a a_a^\dagger a_i + \frac{1}{4} \sum_{abij} t_{ij}^{ab} a_a^\dagger a_b^\dagger a_j a_i$ , and the amplitudes are determined by the nonlinear system of equations  $\langle \Phi_i^a | e^{-T} H e^T | \Phi \rangle = 0$  and  $\langle \Phi_{ij}^{ab} | e^{-T} H e^T | \Phi \rangle = 0$ . The right-hand eigenstates of *H* are then given by

$$|\Psi_0\rangle = e^T |\Phi\rangle \quad (16a)$$

$$|\Psi_n\rangle = \left[ r_0 + \sum_{ai} r_i^a a_a^\dagger a_i + \frac{1}{4} \sum_{abij} r_{ij}^{ab} a_a^\dagger a_b^\dagger a_j a_i \right] e^T |\Phi\rangle \quad (16b)$$

and the left-hand eigenstates ( $n \geq 0$ ) by

$$\langle \tilde{\Psi}_n | = \langle \Phi | \left[ l_0 + \sum_{ai} l_i^a a_i^\dagger a_a + \frac{1}{4} \sum_{abij} l_{ab}^{ij} a_i^\dagger a_j^\dagger a_b a_a \right] e^{-T}. \quad (17)$$

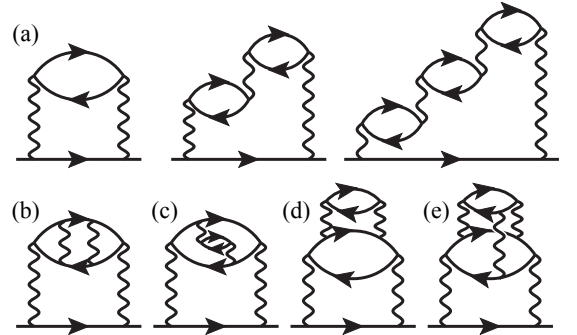


FIG. 1. Example self-energy diagrams included when the polarizability is calculated with EOM-CCSD. The diagrams in (a) are those included in the usual *GW* approximation with RPA screening. Diagram (b) is included with a TDHF polarizability, diagrams (c) and (d) would be included with a BSE polarizability, and diagram (e) – showing an example hole-hole ladder interaction – is only included with the EOM-CCSD polarizability.

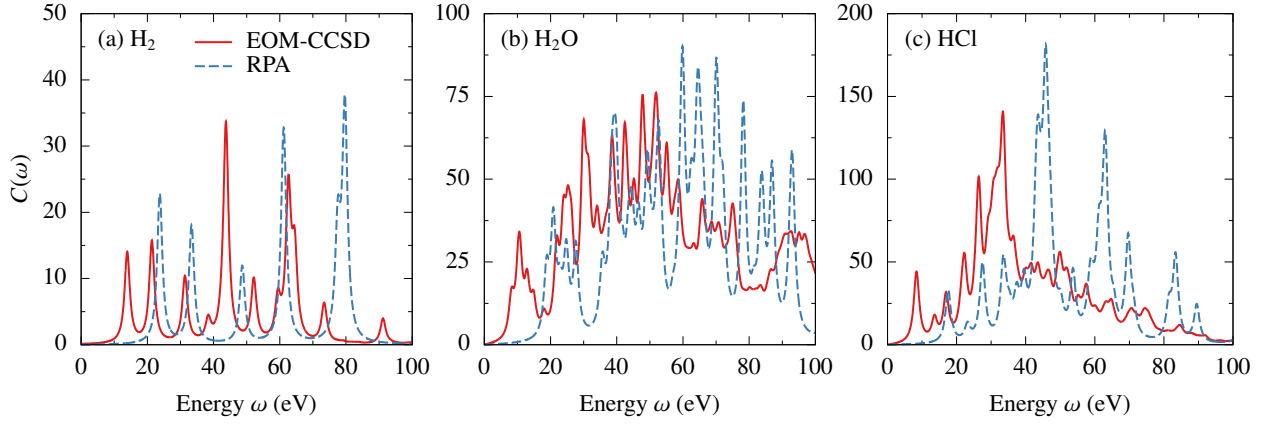


FIG. 2. The spectral function of the polarizability  $C(\omega)$  for  $\text{H}_2$ ,  $\text{H}_2\text{O}$ , and  $\text{HCl}$  calculated using EOM-CCSD and the RPA. All calculations are done in the def2SVP basis using a Hartree-Fock reference and using a numerical broadening of 1 eV.

The transition densities follow naturally

$$\rho_n(\mathbf{x}) = \sum_{pq} \phi_p^*(\mathbf{x}) \phi_q(\mathbf{x}) \langle \tilde{\Psi}_0 | a_p^\dagger a_q | \Psi_n \rangle \quad (18a)$$

$$\rho_n^*(\mathbf{x}) = \sum_{pq} \phi_p^*(\mathbf{x}) \phi_q(\mathbf{x}) \langle \tilde{\Psi}_n | a_p^\dagger a_q | \Psi_0 \rangle, \quad (18b)$$

for which analytic expressions can be simply obtained.<sup>31</sup>

EOM-CCSD is universally viewed as superior to the RPA for electronic excitation energies of molecules. For excited states that are well-described as single excitations, EOM-CCSD is accurate to about 0.1–0.3 eV,<sup>32</sup> whereas the RPA displays errors of 1 eV or more,<sup>33</sup> although a judicious choice of the mean-field reference and inclusion or exclusion of exchange can perform well in specific cases. In a more rigorous sense, the RPA can be derived as an approximation to EOM-CCSD, as recently discussed by one of us.<sup>34</sup> Diagrammatically, the EOM-CCSD polarizability resums all particle-hole ring diagrams (as in the RPA), as well as particle-particle, hole-hole, and particle-hole ladder diagrams, exchange diagrams, and mixtures of all of the above. These extra diagrams define the class of vertex corrections included in the polarizability beyond the RPA. When the RPA or EOM-CCSD polarizability is used in the non-self-consistent  $GW$  approximation, we will term the method the  $G_0W_0$  or  $G_0W_{\text{CC}}$  approximation, respectively. In Fig. 1, we show some example self-energy diagrams included with an EOM-CCSD polarizability, and identify some that are included in various lower levels of theory.

### III. RESULTS

In the results to follow, we study atoms and molecules from the  $GW100$  test set.<sup>12</sup> Due to the relatively high computational cost of obtaining many highly-excited states via EOM-CCSD, we only consider the smallest twenty atoms and molecules, using the polarized double-zeta def2SVP basis set.<sup>35,36</sup> Although we have not optimized the performance, the calculation of ionization potentials with EOM-CCSD vertex corrections in the polarizability can be performed in a manner that

scales as  $N^7$ . By comparing results within a given basis set, our conclusions are largely free of basis set incompleteness error but numerical values should not be compared to experiment or to predictions in other basis sets. All calculations were performed with the PySCF software package.<sup>37</sup>

First, to illustrate the differences between the RPA and EOM-CCSD polarizabilities, we consider the autocorrelation function of the nonlocal density operator  $n(\mathbf{x}, \mathbf{x}') = \sum_{pq} \phi_p(\mathbf{x}) \phi_q^*(\mathbf{x}') a_p^\dagger a_q$ ,

$$\tilde{\Pi}(\mathbf{x}_1, \mathbf{x}'_1, \mathbf{x}_2, \mathbf{x}'_2; \omega) = \int_{-\infty}^{\infty} d(t_1 - t_2) e^{i\omega(t_1 - t_2)} \times \langle \Psi_0 | T[n(\mathbf{x}_1, \mathbf{x}'_1; t_1) n(\mathbf{x}_2, \mathbf{x}'_2; t_2)] | \Psi_0 \rangle, \quad (19)$$

which is related to the usual polarizability by

$$\Pi(\mathbf{x}_1, \mathbf{x}_2; \omega) = \lim_{\substack{\mathbf{x}'_1 \rightarrow \mathbf{x}_1 \\ \mathbf{x}'_2 \rightarrow \mathbf{x}_2}} \tilde{\Pi}(\mathbf{x}_1, \mathbf{x}'_1, \mathbf{x}_2, \mathbf{x}'_2; \omega). \quad (20)$$

In Fig. 2, we show the two-particle spectral function defined by  $C(\omega) = -\pi^{-1} \text{ImTr} \tilde{\Pi}(\omega)$ , for three example molecules,  $\text{H}_2$  (for which EOM-CCSD is exact),  $\text{H}_2\text{O}$  and  $\text{HCl}$ , over a very wide spectral range. RPA and EOM-CCSD calculations are done with a Hartree-Fock (HF) reference; see below for further discussion of this choice. Due to the very slow decay of  $(\omega - E)^{-1}$ , the self-energy at a given frequency is affected by a very large number of neutral excitation energies, as can be inferred from Eq. (11). Indeed, truncating the number of neutral excitation energies retained in the polarizability can affect the ionization potentials (IPs) by anywhere from 0.1 to 1 eV.<sup>38</sup> For all molecules, the RPA spectra are shifted to higher energies by 10 eV or more. This behavior is because the RPA polarizability does not include the electron-hole ladder diagrams that are included in the EOM-CCSD polarizability. These ladder diagrams reduce the excitation energy of molecules and lead to bound exciton states in semiconductors.<sup>28</sup> The overestimation of excitation energies can be partially, but not systematically, alleviated by choosing a mean-field reference with a smaller gap. Compared to HF, essentially all flavors of density functional theory (DFT) satisfy this

property, which explains the popularity of the DFT+RPA approach. Roughly speaking, a larger spectral gap in the polarizability will reduce the screening, such that the  $GW$  correction is less effective and the IPs are too large. However, we will see that this picture is oversimplified, because the residues of the poles of the self-energy also affect the magnitude of the  $GW$  correction. Indeed, despite the smaller spectral gap in the EOM-CCSD polarizability, its use in vertex-corrected  $GW$  calculations will actually predict *even larger* IPs on average.

In Tab. I, we present the first IP of the twenty smallest atoms and molecules of the  $GW100$  test set, obtained via  $G_0W_0$  and  $G_0W_{CC}$ . As a reference, we calculate the first IP using  $\Delta\text{CCSD(T)}$ , i.e. as a difference in ground-state energies between the neutral and charged systems using CCSD with perturbative triple excitations. In all  $GW$  calculations, we use Hartree-Fock (HF) theory as the mean-field reference, which has been established as a good choice for molecules.<sup>11,13,39</sup> Importantly, the HF starting point has no self-interaction error through first order. However, the missing correlation and orbital relaxation leads to HF IPs that are too large in magnitude (orbital energies are too negative). Consistent with previous results,<sup>13</sup> the  $G_0W_0@HF$  approximation predicts reasonably accurate IPs, with a mean error (ME) of +0.187 eV and a mean absolute error (MAE) of 0.314 eV. The vertex-corrected  $G_0W_{CC}@HF$  approximation gives slightly worse results, with a ME of +0.216 eV and a MAE of 0.406 eV. In particular, the vertex-corrected calculations give a less accurate IP for thirteen of the twenty molecules. We also note that for the two-electron molecules  $H_2$  and He, the EOM-CCSD polarizability,

and thus  $W$ , is exact.

As discussed above, the vertex-corrected calculation predicts *larger* IPs than the calculation without (on average), despite the lower – and more accurate – neutral excitation energies in the polarizability. Perhaps even more surprisingly, the IPs only differ by about 0.1 eV, despite the fact that the neutral excitation energies in the polarizability differ by 10 eV or more. Both of these behaviors can be understood from Fig. 3, which shows the frequency dependence of the real part of the self-energy for the highest occupied molecular orbital (HOMO), corresponding to the first IP. The poles of the self-energy with vertex corrections are clearly shifted to higher energies (less negative) by about 10 eV, consistent with the differences in the polarizabilities shown in Fig. 2. However, the pole strengths are also systematically reduced compared to the those of the self-energy without vertex corrections. These two effects cancel one another, such that the IPs are only marginally changed. The example molecules shown demonstrate the three possible cases: in  $H_2$ , the decreased excitation energy is more influential leading to a correct decrease of the IP; in  $H_2O$ , the reduced pole strength is more influential leading to an incorrect increase of the IP; and in  $HCl$ , the two almost exactly cancel leading to a negligible change in the IP.

Although we do not show the detailed results here, we have also implemented vertex corrections at the TDHF level,<sup>15</sup> which can be viewed as intermediate between the RPA (no vertex corrections) and EOM-CCSD. TDHF vertex corrections to the polarizability add particle-hole ladder diagrams – shown in Fig. 1(b) – that are responsible for excitonic effects and expected to be important in molecules. Interestingly, the TDHF excitation energies are much closer to those of EOM-CCSD, but the pole strengths in the self-energy are much closer to those of the RPA. Because of this, the IP with TDHF screening is consistently smaller than that predicted with either RPA or EOM-CCSD screening. However, this choice leads to an overcorrection such that IPs are underestimated, with a mean error of -0.291 eV and a mean absolute error of 0.509 eV. This behavior is demonstrated in Fig. 4, which compares the  $GW$  self energy calculated using the RPA, TDHF, and EOM-CCSD polarizabilities for the  $HCl$  molecule. We conclude that accurate excited-state wavefunctions (i.e. transition densities) are as important as accurate excited-state energies.

These collective results demonstrate that high-quality vertex corrections to the polarizability do not improve the ionization potentials of small molecules within the  $GW$  approximation. Moreover, it appears that the  $G_0W_0$  approximation benefits from a cancellation of errors when vertex corrections to the polarizability are neglected, i.e. errors in the neutral excitation energies are compensated by errors in the pole strength of the self-energy. These findings are qualitatively consistent with previous solid-state calculations, where it was found that adding low-order vertex corrections to the polarizability alone unphysically reduced the bandwidth<sup>23</sup> and increased the work function<sup>40</sup> of simple models of metals, and increased the quasiparticle energy of insulators and semiconductors.<sup>24</sup> It has also been shown that small improvements to the polarizability make little difference to the ionization potentials of atoms.<sup>40</sup>

Molecule	$\Delta\text{CCSD(T)}$	$G_0W_0@HF$	$G_0W_{CC}@HF$	$G_{ev}W_{CC}@HF$
He	24.308	24.32	24.337	24.327
Ne	21.084	20.983	21.534	21.502
$H_2$	16.257	16.245	16.050	16.058
$Li_2$	5.068	5.029	4.909	4.927
LiH	7.692	7.811	7.467	7.351
FH	15.597	15.638	16.072	16.028
Ar	15.199	15.307	15.370	15.355
$H_2O$	12.066	12.267	12.555	12.514
LiF	10.756	10.508	10.651	10.368
HCl	12.148	12.314	12.332	12.220
BeO	9.980	9.632	9.510	9.329
CO	13.700	14.733	14.673	14.629
$N_2$	15.268	16.982	16.735	16.735
$CH_4$	14.247	14.511	14.451	14.433
$BH_3$	13.167	13.416	13.282	13.274
$NH_3$	10.317	10.614	10.730	10.703
BF	10.818	10.977	10.785	10.787
BN	11.888	11.364	11.192	11.183
$SH_2$	9.891	10.069	10.043	10.034
$F_2$	15.563	16.030	16.660	16.580
ME	-	+0.187	+0.216	+0.172
MAE	-	0.314	0.406	0.417

TABLE I. The first ionization potential in eV calculated using  $G_0W_0@HF$ ,  $G_0W_{CC}@HF$ , and  $G_{ev}W_{CC}@HF$ , where EOM-CCSD is used to calculate the screening potential  $W_{CC}$ , compared to a  $\Delta\text{CCSD(T)}$  calculation for reference. All calculations are done in the def2SVP basis using a Hartree-Fock reference.



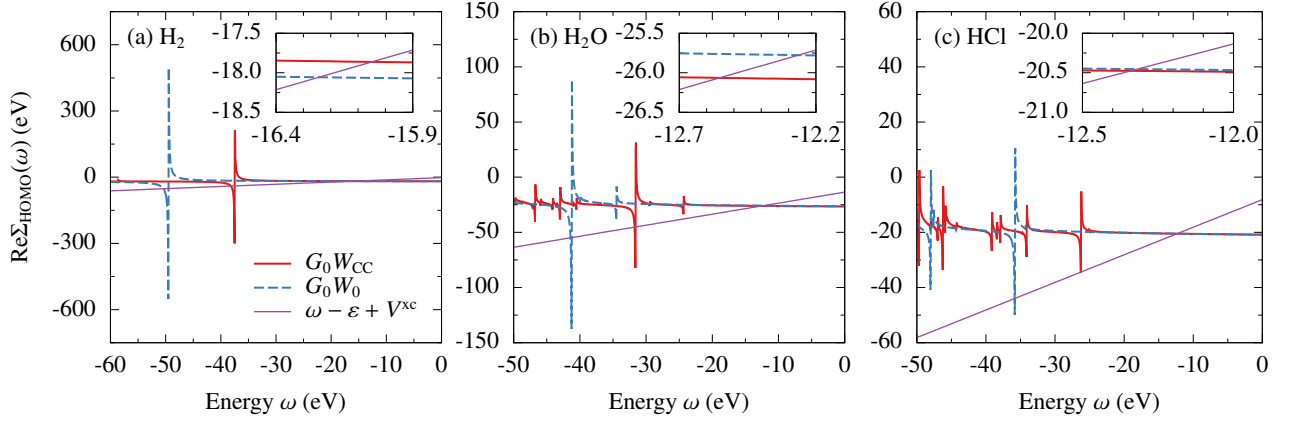


FIG. 3. The real part of the HOMO self-energy for  $\text{H}_2$ ,  $\text{H}_2\text{O}$ , and  $\text{HCl}$  calculated using the vertex-corrected  $G_0W_{\text{CC}}$  and non-vertex-corrected  $G_0W_0$  approximations. Each inset magnifies a  $(0.5 \text{ eV}) \times (1 \text{ eV})$  region around the quasiparticle energies, where  $\Sigma_{\text{HOMO}}(\omega) = \omega - \varepsilon + V^{\text{xc}}$ . The self-energy is calculated with a small imaginary part of  $\eta = 0.03 \text{ eV}$ .

The present work extends these previous results by employing a far more accurate and diagrammatically-defined polarizability, and demonstrating that this trend holds across a range of molecular systems.

Having addressed the low-level RPA treatment of screening, we now consider the two remaining sources of error in the  $GW$  approximation: vertex corrections to the self-energy and self-consistency. The former are more challenging to implement than vertex corrections to the polarizability, however future work will address this issue. While self-consistency is also challenging, one relatively inexpensive option is to enforce eigenvalue self-consistency.<sup>3,41–46</sup> In this approach, the quasiparticle eigenvalues associated with each orbital are replaced with the newly calculated quasiparticle energies after each iteration of the  $GW$  calculation until self-consistency is established. Despite not being fully self-consistent, these methods have been found to significantly reduce the starting point dependence of  $GW$  calculations.<sup>43,45,46</sup> Here, we im-

plement and test eigenvalue self-consistency for EOM-CCSD vertex-corrected  $GW$  calculations.

A major advantage of using EOM-CCSD for vertex corrections is that the coupled-cluster framework is extremely insensitive to the choice of mean-field reference.<sup>47</sup> This can be understood by the Thouless theorem, which shows that the single excitation part of the coupled-cluster wave operator,  $e^{T_1}$ , is able to transform a Slater determinant into any other.<sup>48</sup> This insensitivity is responsible for the common choice of a HF reference, for which the working equations are simpler. In numerical tests, we find that eigenvalue self-consistency makes almost no change to the EOM-CCSD polarizability, and thus we enforce eigenvalue self-consistency in  $G$  only (but the results should be understood as essentially those of complete eigenvalue self-consistency). We refer to this approach as  $G_{\text{ev}}W_{\text{CC}}$ ; the IPs predicted by this method are listed in Tab. I. We find that enforcing eigenvalue self-consistency makes only a very small difference: the IPs calculated using  $G_0W_{\text{CC}}$  and  $G_{\text{ev}}W_{\text{CC}}$  differ by less than 0.1 eV for seventeen of the twenty molecules. While the mean (signed) error has been slightly reduced to +0.172 eV, the mean absolute error has increased to 0.417 eV. We conclude that combining eigenvalue self-consistency with a large class of vertex corrections to the polarizability still does not improve upon the  $G_0W_0$  approximation.

#### IV. CONCLUSION

In this work, we have investigated the effect of high-quality vertex corrections to the polarizability for use in the  $GW$  approximation. Vertex corrections were implemented using EOM-CCSD, which corresponds to an infinite order resummation of particle-hole, particle-particle, and hole-hole ladder diagrams, in addition to the usual ring diagrams, and mixtures of all of the above.<sup>34</sup> The resulting polarizability is undeniably more accurate than that predicted by the RPA. However, the vertex-corrected  $GW$  approximation showed no significant improvement when applied to a test set of twenty small atoms

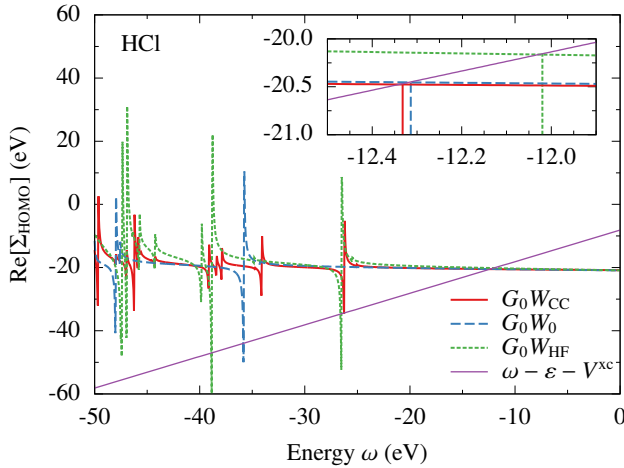


FIG. 4. The same as in Fig. 3(c), but also including the result with TDHF vertex corrections, corresponding to electron-hole interactions in the polarizability.

and molecules. Contrary to expectations, the improved treatment of screening incorrectly increased the ionization potentials on average. Enforcing eigenvalue self-consistency also showed no improvement.

As mentioned above, the only remaining approximation is the neglect of vertex corrections in the self-energy. Without these, the  $GW$  approximation neglects the transient interactions between the screened particle and the particle-hole pairs responsible for screening. Additionally, the neglected exchange diagrams in the self-energy are responsible for a self-screening error.<sup>49,50</sup> However, when the lowest-order vertex corrections to the self-energy were included in the calculation of the bandgaps of silicon<sup>51</sup> and a semiconducting wire,<sup>25</sup> only small improvements were observed. Furthermore, these corrections are found to cancel with the lowest order corrections to the polarizability, as mentioned previously.<sup>21–26</sup> In order to significantly improve upon the  $G_0W_0$  approximation, it appears necessary to include high-order vertex corrections to both the self-energy and the polarizability.

We note that a number of other Green’s function based approaches include infinite-order vertex corrections in both the self-energy and the polarizability, including the two-particle-hole Tamm-Dancoff approximation,<sup>52</sup> the third-order algebraic diagrammatic construction (ADC(3)),<sup>53</sup> and the EOM-CC Green’s function.<sup>54,55</sup> However, most of these methods do not provide the forward and backward time-orderings needed to entirely subsume the conventional RPA; two notable exceptions are the EOM-CC Green’s function with single, double, and triple excitations, as discussed recently in relation to the  $GW$  approximation,<sup>56</sup> and the Faddeev random-phase approximation.<sup>57,58</sup>

All calculations were performed with the PySCF software package,<sup>37</sup> using resources provided by the University of Chicago Research Computing Center. This work was supported by the Air Force Office of Scientific Research under award number FA9550-18-1-0058. T.C.B. is an Alfred P. Sloan Research Fellow.

\* berkelbach@uchicago.edu

- <sup>1</sup> L. Hedin, *Phys. Rev.* **139**, A796 (1965).
- <sup>2</sup> M. S. Hybertsen and S. G. Louie, *Phys. Rev. Lett.* **55**, 1418 (1985).
- <sup>3</sup> M. S. Hybertsen and S. G. Louie, *Phys. Rev. B* **34**, 5390 (1986).
- <sup>4</sup> R. W. Godby, M. Schlüter, and L. J. Sham, *Phys. Rev. B* **37**, 10159 (1988).
- <sup>5</sup> F. Aryasetiawan and O. Gunnarsson, *Rep. Prog. Phys.* **61**, 237 (1998).
- <sup>6</sup> W. G. Aulbur, L. Jönsson, and J. W. Wilkins, *Solid State Phys.* **54**, 1 (2000).
- <sup>7</sup> F. Hüser, T. Olsen, and K. S. Thygesen, *Phys. Rev. B* **87**, 1 (2013).
- <sup>8</sup> Z. Ergonenc, B. Kim, P. Liu, G. Kresse, and C. Franchini, *Phys. Rev. Mater.* **2**, 24601 (2018).
- <sup>9</sup> C. Rostgaard, K. W. Jacobsen, and K. S. Thygesen, *Phys. Rev. B* **81**, 85103 (2010).
- <sup>10</sup> F. Bruneval, *J. Chem. Phys.* **136**, 194017 (2012).
- <sup>11</sup> F. Bruneval and M. a. L. Marques, *J. Chem. Theory Comput.* **9**, 324 (2013).
- <sup>12</sup> M. J. Van Setten, F. Caruso, S. Sharifzadeh, X. Ren, M. Scheffler, F. Liu, J. Lischner, L. Lin, J. R. Deslippe, S. G. Louie, C. Yang, F. Weigend, J. B. Neaton, F. Evers, and P. Rinke, *J. Chem. Theory Comput.* **11**, 5665 (2015).
- <sup>13</sup> F. Caruso, M. Dauth, M. J. van Setten, and P. Rinke, *J. Chem. Theory Comput.* **12**, 5076 (2016).
- <sup>14</sup> L. Hung, F. Bruneval, K. Baishya, and S. Öüt, *J. Chem. Theory Comput.* **13**, 2135 (2017).
- <sup>15</sup> E. Maggio and G. Kresse, *J. Chem. Theory Comput.* **13**, 4765 (2017).
- <sup>16</sup> M. Govoni and G. Galli, *J. Chem. Theory Comput.* **14**, 1895 (2018).
- <sup>17</sup> M. Shishkin, M. Marsman, and G. Kresse, *Phys. Rev. Lett.* **99**, 14 (2007).
- <sup>18</sup> A. Grüneis, G. Kresse, Y. Hinuma, and F. Oba, *Phys. Rev. Lett.* **112**, 096401 (2014).
- <sup>19</sup> W. Chen and A. Pasquarello, *Phys. Rev. B* **92**, 041115 (2015).
- <sup>20</sup> P. S. Schmidt, C. E. Patrick, and K. S. Thygesen, *Phys. Rev. B* **96**, 205206 (2017).
- <sup>21</sup> T. M. Rice, *Ann. Phys. (N. Y.)* **31**, 100 (1965).
- <sup>22</sup> P. Minnhagen, *J. Phys. C Solid State Phys.* **7**, 3013 (1974).
- <sup>23</sup> G. D. Mahan and B. E. Sernelius, *Phys. Rev. Lett.* **62**, 2718 (1989).
- <sup>24</sup> R. Del Sole, L. Reining, and R. W. Godby, *Phys. Rev. B* **49**, 8024 (1994).
- <sup>25</sup> H. de Groot, R. Ummels, P. Bobbert, and W. van Haeringen, *Phys. Rev. B* **54**, 2374 (1996).
- <sup>26</sup> E. L. Shirley, *Phys. Rev. B* **54**, 7758 (1996).
- <sup>27</sup> H. Ma, M. Govoni, F. Gygi, and G. Galli, arXiv:1808.10001 (2018).
- <sup>28</sup> M. Rohlfing and S. G. Louie, *Phys. Rev. B* **62**, 4927 (2000).
- <sup>29</sup> G. Onida, L. Reining, and A. Rubio, *Rev. Mod. Phys.* **74**, 601 (2002).
- <sup>30</sup> P. Ring and P. Shuck, *The Nuclear Many-Body Problem* (Springer-Verlag Berlin Heidelberg, 1980).
- <sup>31</sup> J. F. Stanton and R. J. Bartlett, *J. Chem. Phys.* **98**, 7029 (1993).
- <sup>32</sup> M. Schreiber, M. R. Silva-Junior, S. P. Sauer, and W. Thiel, *J. Chem. Phys.* **128**, 134110 (2008).
- <sup>33</sup> K. B. Wiberg, A. E. De Oliveira, and G. Trucks, *J. Phys. Chem. A* **106**, 4192 (2002).
- <sup>34</sup> T. C. Berkelbach, *J. Chem. Phys.* **149**, 041103 (2018).
- <sup>35</sup> F. Weigend and R. Ahlrichs, *Phys. Chem. Chem. Phys.* **7**, 3297 (2005).
- <sup>36</sup> F. Weigend, *Phys. Chem. Chem. Phys.* **8**, 1057 (2006).
- <sup>37</sup> Q. Sun, T. C. Berkelbach, N. S. Blunt, G. H. Booth, S. Guo, Z. Li, J. Liu, J. D. McClain, E. R. Sayfutyarova, S. Sharma, S. Wouters, and G. K. L. Chan, *Wiley Interdiscip. Rev. Comput. Mol. Sci.* **8**, e1340 (2018).
- <sup>38</sup> F. Bruneval, T. Rangel, S. M. Hamed, M. Shao, C. Yang, and J. B. Neaton, *Comput. Phys. Commun.* **208**, 149 (2016).
- <sup>39</sup> F. Caruso, P. Rinke, X. Ren, M. Scheffler, and A. Rubio, *Phys. Rev. B* **86**, 1 (2012).
- <sup>40</sup> A. J. Morris, M. Stankovski, K. T. Delaney, P. Rinke, P. García-González, and R. W. Godby, *Phys. Rev. B* **76**, 1 (2007).
- <sup>41</sup> Y. Pavlyukh and W. Hübner, *Phys. Lett. A* **327**, 241 (2004).
- <sup>42</sup> X. Blase, C. Attaccalite, and V. Olevano, *Phys. Rev. B* **83**, 1 (2011).
- <sup>43</sup> C. Faber, C. Attaccalite, V. Olevano, E. Runge, and X. Blase, *Phys. Rev. B* **83**, 1 (2011).
- <sup>44</sup> N. Marom, F. Caruso, X. Ren, O. T. Hofmann, T. Körzdörfer, J. R.

- Chelikowsky, A. Rubio, M. Scheffler, and P. Rinke, *Phys. Rev. B* **86**, 1 (2012).
- <sup>45</sup> F. Kaplan, F. Weigend, F. Evers, and M. J. Van Setten, *J. Chem. Theory Comput.* **11**, 5152 (2015).
- <sup>46</sup> F. Kaplan, M. E. Harding, C. Seiler, F. Weigend, F. Evers, and M. J. Van Setten, *J. Chem. Theory Comput.* **12**, 2528 (2016).
- <sup>47</sup> I. Shavitt and R. J. Bartlett, *Many-Body Methods in Chemistry and Physics: MBPT and Coupled-Cluster Theory* (Cambridge University Press, Cambridge; New York, 2009).
- <sup>48</sup> D. J. Thouless, *Nucl. Phys.* **21**, 225 (1960).
- <sup>49</sup> P. Romaniello, S. Guyot, and L. Reining, *J. Chem. Phys.* **131**, 154111 (2009).
- <sup>50</sup> J. Wetherell, M. J. P. Hodgson, and R. W. Godby, *Phys. Rev. B* **97**, 121102 (2018).
- <sup>51</sup> P. A. Bobbert and W. Van Haeringen, *Phys. Rev. B* **49**, 10326 (1994).
- <sup>52</sup> O. Walter and J. Schirmer, *J. Phys. B At. Mol. Phys.* **14**, 3805 (1981).
- <sup>53</sup> J. Schirmer, L. S. Cederbaum, and O. Walter, *Phys. Rev. A* **28**, 1237 (1983).
- <sup>54</sup> M. Nooijen and J. G. Snijders, *Int. J. Quantum Chem. Quantum Chem. Symp.* **83**, 55 (1992).
- <sup>55</sup> M. Nooijen and J. G. Snijders, *Int. J. Quantum Chem.* **48**, 15 (1993).
- <sup>56</sup> M. F. Lange and T. C. Berkelbach, *J. Chem. Theory Comput.* **14**, 4224 (2018).
- <sup>57</sup> C. Barbieri, D. Van Neck, and W. H. Dickhoff, *Phys. Rev. A* **76**, 1 (2007).
- <sup>58</sup> M. Degroote, D. Van Neck, and C. Barbieri, *Phys. Rev. A* **83**, 042517 (2011).